ORIGINAL RESEARCH

Rac1 Signaling Is Critical to Cardiomyocyte Polarity and Embryonic Heart Development

Carmen Leung, BMSc; Xiangru Lu, MD; Murong Liu, RN; Qingping Feng, MD, PhD

***Background*—**Defects in cardiac septation are the most common form of congenital heart disease, but the mechanisms underlying these defects are still poorly understood. The small GTPase Rac1 is implicated in planar cell polarity of epithelial cells in *Drosophila*; however, its role in mammalian cardiomyocyte polarity is not clear. We tested the hypothesis that Rac1 signaling in the second heart field regulates cardiomyocyte polarity, chamber septation, and right ventricle development during embryonic heart development.

***Methods and Results*—**Mice with second heart field–specific deficiency of *Rac1* (*Rac1*^{SHF}) exhibited ventricular and atrial septal defects, a thinner right ventricle myocardium, and a bifid cardiac apex. Fate-mapping analysis showed that second heart field contribution to the interventricular septum and right ventricle was deficient in *Rac1*^{SHF} hearts. Notably, cardiomyocytes had a spherical shape with disrupted F-actin filaments in *Rac1*^{SHF} compared with elongated and well-aligned cardiomyocytes in littermate controls. Expression of Scrib, a core protein in planar cell polarity, was lost in *Rac1*^{SHF} hearts with decreased expression of *WAVE* and *Arp2/3*, leading to decreased migratory ability. In addition, Rac1-deficient neonatal cardiomyocytes displayed defects in cell projections, lamellipodia formation, and cell elongation. Furthermore, apoptosis was increased and the expression of *Gata4*, *Tbx5*, *Nkx2.5*, and *Hand2* transcription factors was decreased in the *Rac1*^{SHF} right ventricle myocardium.

***Conclusions*—**Deficiency of Rac1 in the second heart field impairs elongation and cytoskeleton organization of cardiomyocytes and results in congenital septal defects, thin right ventricle myocardium, and a bifid cardiac apex. Our study suggests that Rac1 signaling is critical to cardiomyocyte polarity and embryonic heart development. **(*J Am Heart Assoc*. 2014;3:e001271 doi: 10.1161/JAHA.114.001271)**

Key Words: congenital heart defects • heart septal defects • Rac1 • second heart field

Adult cardiomyocytes are highly polarized, with a rod shape and the majority of their cell junction proteins localized to the intercalated discs joining the cells end to end to facilitate electrical conduction and contraction of the heart[1]; however, during embryonic development, cardiomyocytes are initially formed in spherical shapes. They begin to elongate at E13.5 and gradually assume a rod shape during fetal and postnatal development. The spatial differences or asymmetries in shape, orientation and structure of cells define cell polarity, which is controlled by planar cell polarity (PCP) signaling, also known as the noncanonical Wnt pathway.[2] Initially identified in *Drosophila*, the PCP pathway is well conserved in mammalian species.[1,3] The ligands of this pathway include Wnt5a and Wnt11. The transmembrane receptors involved are Frizzled and Vangl2/Scrib. Through recruitment of Dishevelled, the PCP signals are transduced to the small GTPases RhoA and Rac, which in turn regulate actin polymerization and cell polarity.[1,2] The important role of PCP signaling in regulating cardiomyocyte polarity and embryonic heart development has recently emerged. Genetic knockout or mutation of PCP components such as *Wnt11*, *Vangl2*, *Scrib*, and *Dishevelled2* in mice all show congenital heart defects (CHDs).[4–6] In addition, *Wnt11*$^{-/-}$ and *Vangl2* mutant mice show thin myocardium and defects in cardiomyocyte elongation, organization, and migration[4,5]; however, the role of Rac in cardiomyocyte polarity and embryonic heart development is unknown.

Rac GTPases are small (20 to 30 kDa), monomeric, signaling GTP-binding proteins that are a subfamily of the

From the Departments of Physiology and Pharmacology (C.L., X.L, Q.F.), Medicine (Q.F.), Schulich School of Medicine and Dentistry, Collaborative Program in Developmental Biology (C.L.), Lawson Health Research Institute (M.L., Q.F.), The University of Western Ontario, London, Ontario, Canada N6A 5C1.

Correspondence to: Qingping Feng, MD, PhD, Department of Physiology and Pharmacology, Schulich School of Medicine and Dentistry, University of Western Ontario, London, Ontario, Canada N6A 5C1. E-mail: qingping.feng@schulich.uwo.ca

Received August 19, 2014; accepted September 15, 2014.

Rho family of GTPases with 4 members: Rac1, Rac2, Rac3, and RhoG.[7] Rac1 is a key molecule in the PCP pathway to promote cell polarity of the eyes and wings in *Drosophila*.[8,9] Rac1 is also an important regulator of cell migration and survival. Whole-body *Rac1*$^{-/-}$ mice die before E9.5, with defects in germ layer formation due to reduced cell adhesion and motility and increased apoptosis within the mesoderm.[10] Moreover, *Rac1*$^{-/-}$ embryos fail to specify an anterior–posterior axis because cells in the anterior visceral endoderm do not migrate,[11] suggesting an important role of Rac1 in cell polarity during embryogenesis.

The heart develops from 3 distinct populations of cells: the first heart field, the second heart field (SHF), and the cardiac neural crest. Initially, the primary heart tube is formed mainly from the first heart field progenitors. SHF cells are then added to the heart tube to form the right ventricle (RV) and the outflow tract, with contributions from the cardiac neural crest cells.[12,13] In addition, SHF progenitors are critical to the formation of the cardiac septum. Abnormalities in SHF development result in CHDs in mice including septal defects, which are some of the most common types of CHDs in humans.[14,15] To specifically study the role of Rac1 in cardiomyocyte polarity and RV and cardiac septal development, we generated a novel mouse model with an SHF-specific (or anterior heart field-specific) deficiency of *Rac1* (*Rac1*^{SHF}) using the *Mef2c-Cre* mouse, which directs Cre activity in the SHF.[16] Our results show that Rac1 signaling in the SHF is critical to cardiomyocyte polarity, cardiac septation, and RV development.

Methods

Mice

Rac1$^{f/f}$ mice (stock no. 5550)[17] and membrane-targeted Tomato (mT)/membrane-targeted green fluorescent protein (mG) mice (stock no. 7676)[18] were obtained from Jackson Laboratory (Bar Harbor, Maine). The *mT/mG* mouse is a global double-fluorescent Cre reporter mouse that expresses mT before Cre-excision and mG after excision of mT.[18] The *Mef2c-Cre* embryos[16] were obtained from Mutant Mouse Regional Resource Centers (Chapel Hill, North Carolina) and rederived. A breeding program was carried out to generate *Mef2c-Cre:Rac1*$^{f/f}$ (*Rac1*^{SHF}), *Mef2c-Cre:mT/mG*, and *Rac1*^{SHF}*:mT/mG* transgenic mice. Genotyping was performed by polymerase chain reaction (PCR) using genomic DNA from tail biopsies. Primer sequences are shown in Table 1. All mouse experiments and procedures were carried out in accordance with the guidelines of the Canadian Council of Animal Care and approved by the animal use subcommittee at the University of Western Ontario.

Table 1. The Genotyping Polymerase Chain Reaction Primer Sequences

Gene	Forward	Reverse
Mef2c-Cre	tgccacgaccaagtgacagc	ccaggttacggatatagttcatg
Rac1$^{f/f}$	tccaatctgtgctgcccatc	gatgcttctaggggtgagcc
mT/mG	ctctgctgcctcctggcttct	cgaggcggatcacaagcaata Mutant reverse: tcaatgggcgggggtcgtt

Histological Analysis

Neonatal and embryonic samples were fixed overnight in 4% paraformaldehyde at 4°C, dehydrated, and paraffin embedded. Embryos were serially sectioned at 5 μm from the top of the aortic arch to the apex with a Leica RM2255 microtome. Sections were mounted onto positively charged albumin/glycerin-coated microslides in a set of 5, with 25-μm intervals between each section. Slides were stained with hematoxylin and eosin for histological analysis. Images were captured using a light microscope (Observer D1, Zeiss).

Immunohistochemistry

Immunohistochemical staining was performed on heart sections (5 μm). Antigen retrieval was carried out in sodium citrate buffer (pH 6.0) at 92°C using a BP-111 laboratory microwave (Microwave Research and Applications). Immunostaining was performed with primary antibodies for Rac1 (Santa Cruz Biotechnology), phosphohistone-H3 (phospho S10) (Abcam), cleaved caspase-3 (Cell Signaling Technology), active (non-phosphorylated) β-catenin (Cell Signaling Technology), and green fluorescent protein (Abcam). All slides were imaged with a Zeiss Observer D1 microscope using AxioVision Rel 4.7 software. For phalloidin and wheat germ agglutinin staining, P0 heart samples were fixed in 4% paraformaldehyde, cryoprotected in 30% sucrose, embedded in FSC22 frozen section media (Leica), and sectioned with a Leica cryostat at 10-μm thick onto glass slides. Slides were incubated with Alexa Fluor 488 phalloidin (Life Technologies), Alexa Fluor 647 wheat germ agglutinin (Invitrogen), and Hoechst 33342 (Invitrogen). Confocal images were obtained with a Zeiss LSM 510 Duo microscope using ZEN 2012 software (Zeiss).

Western Blot Analysis

Rac1 protein expression from P0 RV was measured by Western blot analysis. Briefly, 40 μg of protein from isolated RV tissue was separated by 12% SDS-PAGE gel and transferred to nitrocellulose membranes. Blots were probed with antibodies against Rac1 (1:500; Santa Cruz Biotechnology) and GAPDH

(1:3000; Santa Cruz Biotechnology). Blots were then washed and probed with horseradish peroxidase–conjugated secondary antibodies (1:2500; Bio-Rad) and detected using an enhanced chemiluminescence detection method. Signal quantification was performed by densitometry.

RV Explant Culture

Embryos were harvested at E12.5, and embryonic hearts were dissected to separate RV tissue from the whole heart. RV tissues were cultured on 1% collagen-coated tissue culture plastic multiwell plates, as described previously[19] with the following adaptations. Explants were incubated for 6 days at 37°C with 5% CO_2 in DMEM containing 10% fetal bovine serum and 1% penicillin/streptomycin. Media was refreshed every 2 days.

Quantitative Reverse Transcription PCR

Total RNA was isolated from E13.5 RV using the RNeasy Mini Kit (Qiagen). Reverse transcription reaction was performed using M-MLV reverse transcriptase (Invitrogen), and EvaGreen qPCR Mastermix (Applied Biological Materials) was used for real-time thermal cycling. Samples were amplified for 35 cycles using the Eppendorf Mastercycler Realplex Real-Time PCR machine. In addition, 28S ribosomal RNA was used as an internal control. Primer sequences are shown in Table 2. The mRNA levels in relation to 28S ribosomal RNA were determined using a comparative C_T method.[20]

Scratch Assay

Wild-type neonatal cardiomyocytes were prepared and cultured, as described previously.[21] Cardiomyocytes were infected with adenoviruses expressing a dominant-negative form of Rac1 (Ad-Rac1N17; Vector Biolabs) or β-galactosidase (Ad-β-gal; Vector Biolabs) as a control at a multiplicity of infection of 10 plaque forming units per cell. The scratch was

Table 2. The Real-Time Reverse Transcription Polymerase Chain Reaction Primer Sequences

Gene	Forward	Reverse
Arp2	ggcttttctctccctcacct	gcttctgctcctgctcaata
Arp3	cggcgtcctctctacaagaa	cagcattgaccctccaaacc
Abi1	ttgactccacagatccctctcac	ttcatagtccacaggaggaggtg
WAVE2	gcaaggaagagtgggagaagatg	cagagaatgaaggggaaggtgag
Nkx2.5	tcaatgcctatggctacaacg	gacgccaaagttcacgaagttgct
Gata4	cactatgggcacagcagctc	gcctgcgatgtctgagtgac
Tbx5	acacaggatgtctcggatgc	gttaggtgggggcagaaggt
Rac1	aacctgcctgctcatcagtt	ttgtccagctgtgtcccata
Tbx20	cacctatggggaagaggatgttc	gtcgctatggatgctgtactggt
Hand2	gctacatcgcctacctcatggat	tcttgtcgttgctgctcactgt
28S	ttgaaaatccgggggagag	acattgttccaacatgccag

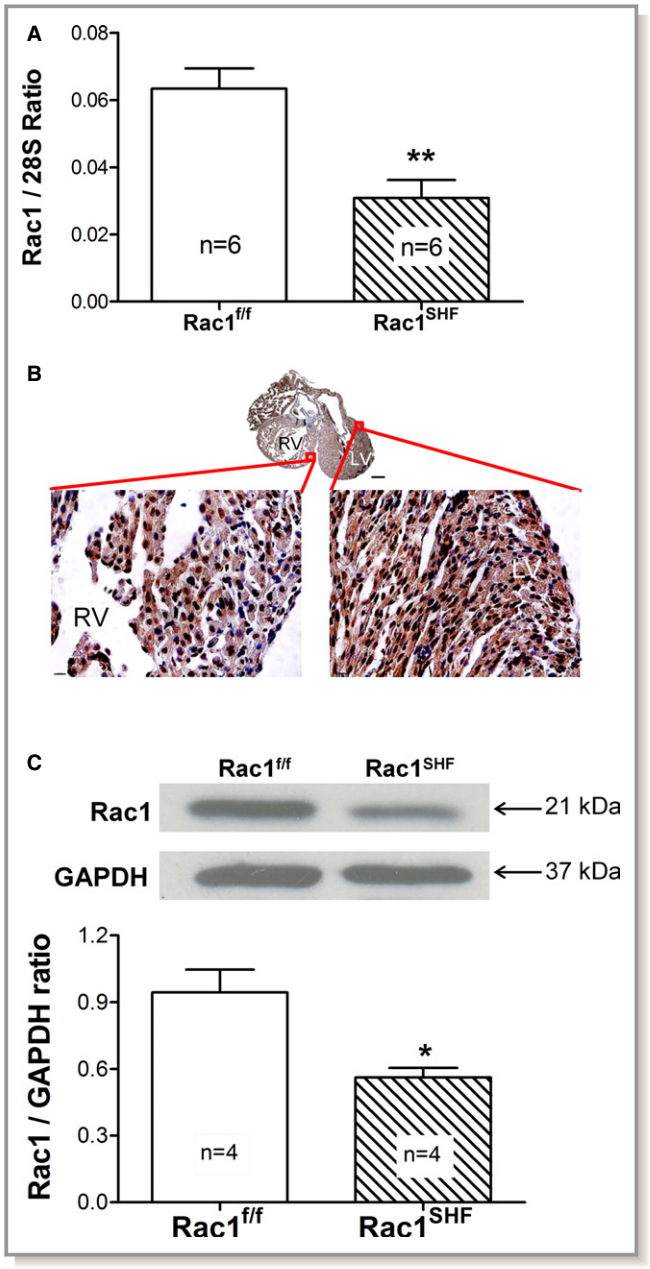

Figure 1. A, *Rac1* mRNA levels were significantly decreased in $Rac1^{SHF}$ RV compared with $Rac1^{f/f}$ controls at E13.5, as measured by quantitative reverse transcription polymerase chain reaction. $^{**}P<0.01$ by unpaired Student *t* test. B, Immunostaining shows that Rac1 protein levels were reduced in P0 $Rac1^{SHF}$ RV compared with the left ventricle myocardium. C, Western blot analysis of P0 RV showed a significant decrease in Rac1 protein in $Rac1^{SHF}$ compared with $Rac1^{f/f}$ controls. $^{*}P<0.05$ by Mann–Whitney test. RV indicates right ventricle; SHF, second heart field.

Table 3. Incidence of Congenital Heart Defects in P0 *Rac1*^{SHF} Hearts

	Rac1$^{f/f}$ (n=19)		Mef2c-Cre:Rac1$^{f/+}$ (n=10)		Rac1^{SHF} (n=28)*	
	n	%	n	%	n	%
Normal	19	100	10	100	0	0
ASD	0	0	0	0	23	82
VSD	0	0	0	0	28	100
Bifid apex	0	0	0	0	28	100
Defective RV	0	0	0	0	28	100

ASD indicates atrial septal defect; RV, right ventricle; VSD, ventricular septal defect.
*21 alive and 7 collected dead at P0. Because penetrance of congenital heart defects is 100% in Rac1^{SHF} hearts, statistical analysis is not necessary.

performed 6 hours after adenoviral infection. Cells were fixed and immunostained with primary antibodies for Rac1 (Santa Cruz Biotechnologies) and α-actinin (Sigma-Aldrich) 24 hours after scratch.

Statistical Analysis

Data are mean±SEM. Unpaired Student *t* test was used when data passed a normality test. Nonparametric Mann–Whitney test was used when samples size was 3 to 4 per group. Differences were considered significant at $P \leq 0.05$.

Results

Generation of a Transgenic Mouse With *Rac1* Knockdown in the SHF

To elucidate the role of *Rac1* in the SHF, the *Mef2c-Cre* mouse was crossed with the *Rac1*$^{f/f}$ mouse to generate *Mef2c-Cre:Rac1*$^{f/f}$ (*Rac1*^{SHF}) offspring. *Rac1*^{SHF} mice have the *Rac1* gene specifically knocked down in SHF progenitors and their derivatives. Embryonic samples were collected, and loss of the *Rac1* transcript was confirmed in *Rac1*^{SHF} hearts by quantitative reverse-transcription PCR. *Rac1* mRNA expression was reduced by 51% in the RV myocardium of E13.5 *Rac1*^{SHF} compared with littermate *Rac1*$^{f/f}$ controls (Figure 1A). Immunostaining for Rac1 protein was also performed to further confirm the loss of myocardial *Rac1* expression in SHF derivatives. In P0 *Rac1*^{SHF} hearts, robust staining for Rac1 was observed in the left ventricle (LV). In the same P0 *Rac1*^{SHF} heart section, the Rac1 signal intensity was markedly decreased in the RV when compared with the LV (Figure 1B). Ratio of Rac1 to GAPDH protein was reduced by 40% in P0 *Rac1*^{SHF} RV compared with littermate *Rac1*$^{f/f}$ controls, as determined by Western blot analysis (Figure 1C). These data show that the *Mef2c-Cre*–mediated recombination downregulates *Rac1* expression in SHF derivatives of the embryonic heart.

Deficiency of *Rac1* in the SHF Results in CHDs

The most prominent defect on initial analysis of P0 *Rac1*^{SHF} hearts was a gross morphological abnormality in the overall shape of the heart. Instead of a distinct apex, all P0 *Rac1*^{SHF} hearts (28 of 28) had a deep interventricular groove and bifurcation of the 2 ventricles, resulting in a bifid cardiac apex, a rare CHD in humans (Table 3; Figure 2A and 2B). Atrial septal defects were observed in 82% (23 of 28) of *Rac1*^{SHF} hearts but not in littermate control *Rac1*$^{f/f}$ P0 hearts (0 of 19) (Table 3; Figure 2C and 2D). Ventricular septal defects were seen in 100% (28 of 28) of P0 *Rac1*^{SHF} hearts (Table 3; Figure 2C and 2D). In addition, the RV myocardium had poor trabeculation and the compact myocardium was significantly thinner in *Rac1*^{SHF} hearts compared with littermate controls (Figure 2E through 2G; Table 3). These findings suggest a critical role for SHF *Rac1* signaling in cardiac septation and RV development.

Rac1^{SHF} Hearts Exhibit Defective Cardiomyocyte Polarity

Cardiomyocyte organization and alignment were severely disrupted in P0 *Rac1*^{SHF} hearts. Cell membrane staining with wheat germ agglutinin revealed rounded, spherically shaped cardiomyocytes in *Rac1*^{SHF} RV (Figure 3B) compared with *Rac1*$^{f/f}$ RV, which had elongated cardiomyocytes (Figure 3A). Actin cytoskeleton organization was also severely disrupted in *Rac1*^{SHF} RV, as shown by phalloidin staining to mark F-actin filaments (Figure 3D). *Rac1*^{SHF} RV had an absence of long F-actin filaments, whereas *Rac1*$^{f/f}$ RV myocardium exhibited long, parallel running F-actin fibers (Figure 3C). In addition, active (nonphosphorylated) β-catenin staining between cell junctions was also reduced in E13.5 *Rac1*^{SHF} RV compared

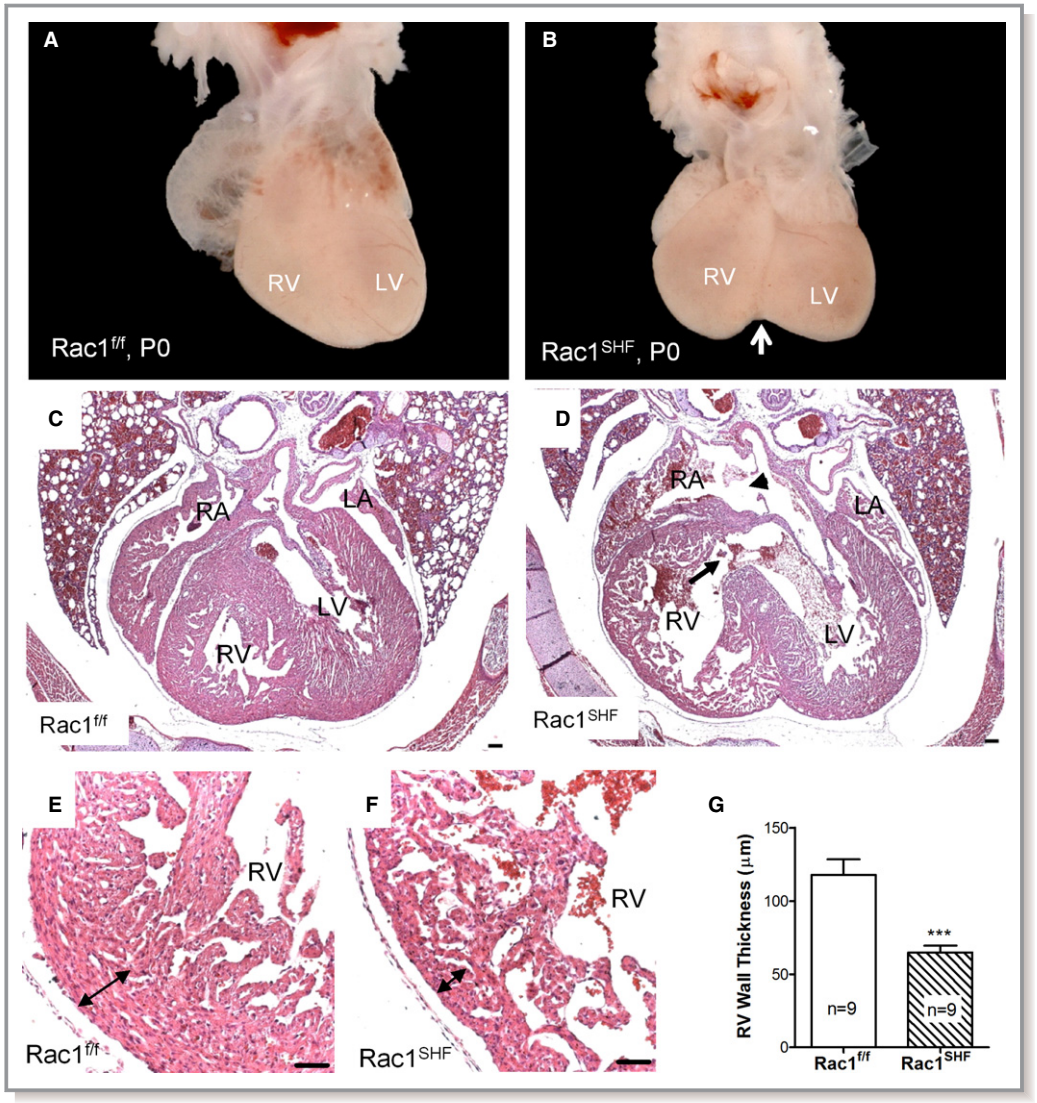

Figure 2. *Mef2c-Cre*–induced *Rac1* deletion in SHF results in congenital heart defects. A and B, Bifurcation between RV and LV (arrow) in P0 $Rac1^{SHF}$ hearts. C and D, Atrial septal defect (arrow head) and ventricular septal defect (arrow) were found in P0 $Rac1^{SHF}$ hearts. E through G, P0 $Rac1^{SHF}$ RV compact myocardium (double arrows) was significantly thinner. ***$P<0.001$ by unpaired Student *t* test. Scale bars: 100 μm (C and D), 50 μm (E and F). LA indicates left atrium; LV, left ventricle; RA, right atrium; RV, right ventricle; SHF, second heart field.

with $Rac1^{f/f}$ RV (Figure 3E and 3F). These data strongly suggest disruption of cardiomyocyte polarity in $Rac1^{SHF}$ hearts.

Expression of Scrib Protein Is Lost in $Rac1^{SHF}$ Hearts

Scrib, the mouse homolog of the *Drosophila* protein Scribble, is a component of the PCP pathway. Immunostaining shows Scrib protein was expressed mainly in the lower part of RV and the cardiac apex in $Rac1^{f/f}$ hearts (Figure 4A, 4B, 4E, and 4F), and the number of Scrib-positive cells was about 10 times higher in E15.5 than E12.5 $Rac1^{f/f}$ hearts (Figure 4I and 4J). Notably, Scrib expression was almost absent in both E12.5 and E15.5 $Rac1^{SHF}$ hearts (Figure 4C, and 4D, 4G, and 4H), and the number of Scrib-positive cells was significantly decreased in $Rac1^{SHF}$ hearts compared with littermate controls (Figure 4I and 4J). The loss of Scrib expression suggests disruption of the PCP pathway and further supports failure to establish cardiomyocyte polarity in $Rac1^{SHF}$ hearts.

Rac1 Is Required for Lamellipodia Formation and Cardiomyocyte Migration

Cell migration is a fundamental process of gastrulation, morphogenesis, and formation of organs and tissues during

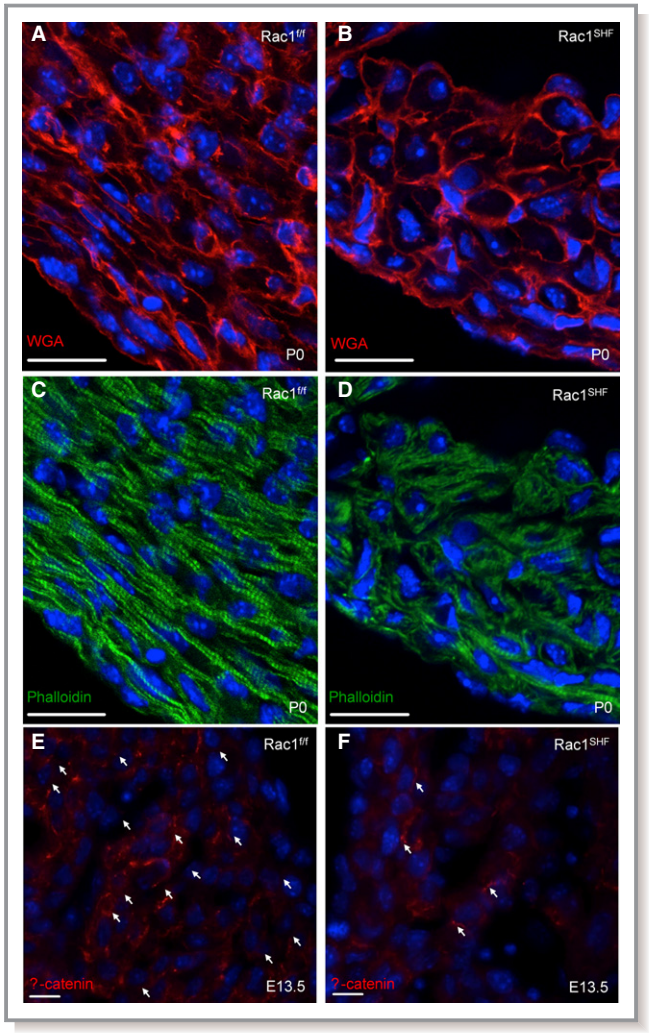

Figure 3. *Rac1*^{SHF} hearts exhibit defective polarity. A and B, WGA staining to mark cell membranes of P0 *Rac1*^{SHF} RV shows rounded cardiomyocytes compared with the elongated cells of littermate controls. C and D, Phalloidin staining to mark F-actin shows disorganization in cellular structure and a deficiency in long actin filaments in the *Rac1*^{SHF} RV. E and F, Active (nonphosphorylated) β-catenin staining is reduced at cell–cell junctions in E13.5 *Rac1*^{SHF} RV. White arrows indicate cell adhesion. Scale bars: 20 μm (A through D), 10 μm (E and F). RV indicates right ventricle; SHF, second heart field; WGA, wheat germ agglutinin.

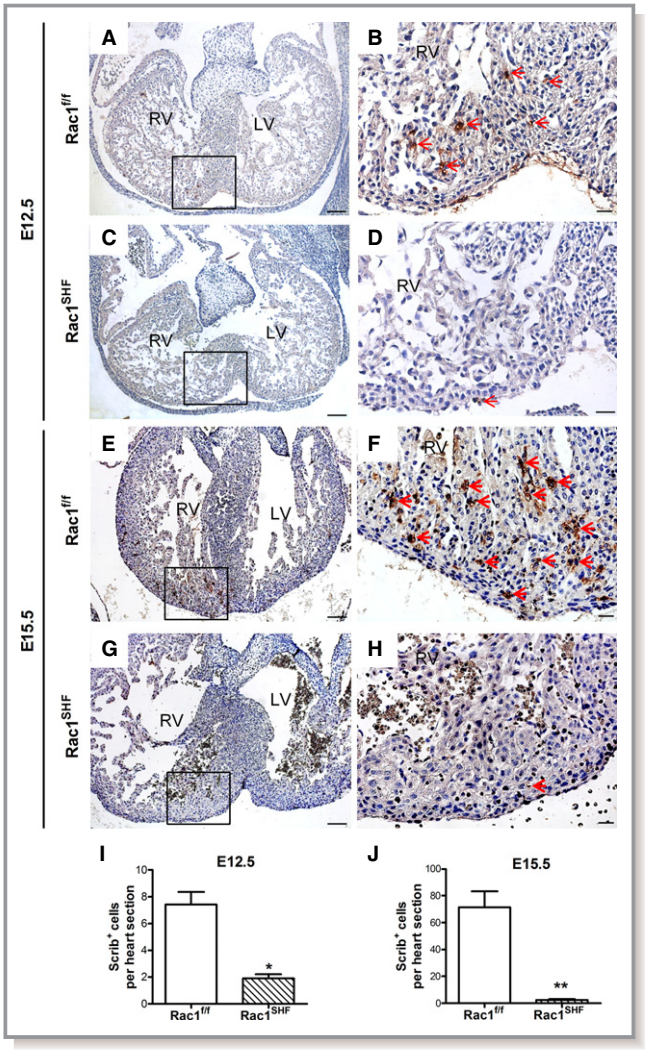

Figure 4. Decreased Scrib protein expression in *Rac1*^{SHF} hearts. A through D, Scrib immunostaining was performed on E12.5 paraffin sections. Arrows indicate Scrib protein expression. B and D are magnifications of boxes in A and C, respectively. E through H, Scrib immunostaining was performed on E15.5 paraffin sections. Arrows indicate Scrib protein expression. F and H are magnifications of boxes in E and G, respectively. I, J, Number of Scrib-positive cells was significantly decreased in E12.5 and E15.5 *Rac1*^{SHF} hearts. n=3 hearts per group, **P*=0.05 by Mann–Whitney test. Scale bars: 100 μm (A, C, E, G), 20 μm (B, D, F, H). LA indicates left atrium; LV, left ventricle; RV, right ventricle; SHF, second heart field.

development.[22] To determine whether Rac1 plays a migratory role in SHF derived-cells, RV from E12.5 *Rac1*^{SHF}:mT/mG and control *Mef2c-Cre:Rac1*$^{f/+}$:mT/mG hearts were isolated and explants cultured on collagen gels for 6 days. The mT/mG global double-fluorescent Cre reporter mouse expresses mT before Cre-mediated excision and mG after excision of mT.[18] Thus all SHF-derived cells in *Rac1*^{SHF}:mT/mG and *Mef2c-Cre:Rac1*$^{f/+}$:mT/mG are positive for green fluorescent protein. It was observed that *Mef2c-Cre:Rac1*$^{f/+}$:mT/mG control explants had both non-SHF-derived (mT-labeled) and SHF-derived (mG-labeled) cells migrating from the RV explant by day 6 (Figure 5A through 5C). In contrast, *Rac1*^{SHF}:mT/mG explants had only non-SHF-derived (mT-labeled) cells migrating from the RV explant and very few to no SHF-derived (mG-labeled) cell migration (Figure 5D through 5F). The migration defects observed in the *Rac1*^{SHF}:mT/mG RV explants indicate that *Rac1* regulates migration of SHF-derived progenitor cells, likely through actin organization controlled by the Wiskott-Aldrich syndrome protein

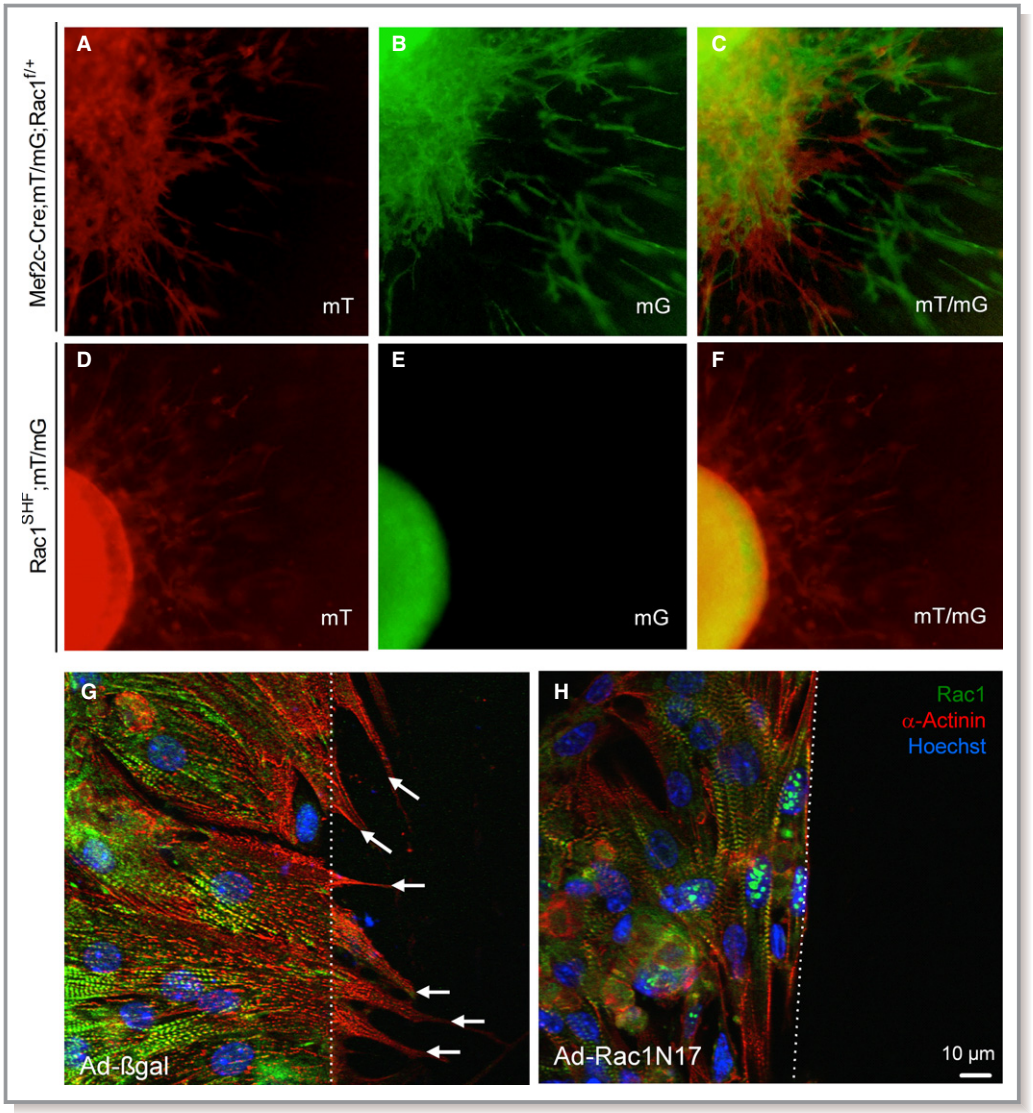

Figure 5. Rac1 deficiency results in defective cell migration and lamellipodia formation. A through C, E12.5 RV explant cultures of *Mef2c-Cre;*mT/mG*;Rac1*$^{f/+}$ hearts have both SHF-derived (mG) and non-SHF-derived (mT) migrating cells. E and F, E12.5 RV explant cultures of *Rac1*^{SHF}*;*mT/mG hearts have only non-SHF-derived (mT) migrating cells without any SHF-derived migrating cells (mG). G and H, Scratch assays of adenoviral infected neonatal cardiomyocytes show cellular projections and lamellipodia extensions (arrows) beyond the scratch edge in Ad-β-gal treated cells and none in Ad-Rac1N17 treated cells 24 hours post-scratch. Dotted white line indicates scratch edge. Shown are representative images from 3 independent experiments. Ad-Rac1N17 indicates a dominant-negative form of Rac1; Ad-β-gal, β-galactosidase; mG, membrane-targeted green fluorescent protein; mT, membrane-targeted Tomato; RV, right ventricle SHF, second heart field.

family verprolin-homologous protein (WAVE) and actin-related protein-2/3 (Arp2/3) pathway downstream of Rac1.[23] A significant decrease was found in *Abi1*, *WAVE2*, *Arp2*, and *Arp3* expression—components of the WAVE and Arp2/3 complex—in E13.5 *Rac1*^{SHF} RV compared with littermate controls (Table 4).

To further assess cell migration, scratch assays were performed on neonatal cardiomyocytes infected with adenoviral constructs of β-galactosidase (Ad-β-gal) or dominant negative Rac1 (Ad-Rac1N17). It was observed that 24 hours after scratch, Ad-β-gal-treated cardiomyocytes were aligned perpendicular to the scratch edge and had projections along the scratch edge, indicative of actin organization and lamellipodia extension (Figure 5G). In contrast, no projections and lamellipodia formation were observed in Ad-Rac1N17 cardiomyocytes, and the cells were disorganized and arranged in a random orientation along the scratch edge (Figure 5H). These findings implicate Rac1 in the regulation

Table 4. Real-Time Polymerase Chain Reaction Analysis of Gene mRNA Levels in E13.5 *Rac1*^{SHF} Right Ventricle

Gene	*Rac1*$^{f/f}$	*Rac1*^{SHF}	*P* Values
Nkx2.5	0.0583±0.00423 (n=6)	0.0462±0.00467 (n=6)	0.0320
Gata4	0.0410±0.00206 (n=6)	0.0299±0.00405 (n=6)	0.0338
Tbx5	0.0124±0.00043 (n=8)	0.0090±0.00135 (n=8)	0.0320
Hand2	0.0315±0.00281 (n=6)	0.0211±0.00116 (n=6)	0.0065
Tbx20	0.0428±0.0038 (n=6)	0.0331±0.00423 (n=8)	0.1256
Abi1	0.0268±0.00215 (n=8)	0.0177±0.00341 (n=8)	0.0404
WAVE2	0.1174±0.00902 (n=8)	0.0756±0.0140 (n=8)	0.0247
Arp2	0.0246±0.00239 (n=8)	0.0167±0.00109 (n=8)	0.0098
Arp3	0.1306±0.00639 (n=8)	0.0901±0.0109 (n=8)	0.0063
β-*actin*	0.2977±0.0395 (n=6)	0.2220±0.0298 (n=6)	0.1534

Data are ratios to 28S and are presented as mean±SEM. Significance in gene expression difference between *Rac1*^{SHF} and *Rac1*$^{f/f}$ littermates analyzed by unpaired Student *t* test. $P<0.05$ was considered statistically significant. No significant differences were found in *Tbx20* and β-*actin* mRNA expression.

of cell migration and lamellipodia extension in cardiomyocytes.

Rac1^{SHF} Cardiomyocytes Are Shortened and Rounded

Neonatal cardiomyocyte cultures from *Rac1*^{SHF} RV tissues showed that these cells had disrupted actin organization, as indicated by phalloidin staining and the absence of distinct cell projections compared with *Rac1*$^{f/f}$ cardiomyocytes. Interestingly, patterning of α-actinin also seemed to be disrupted in *Rac1*^{SHF} cardiomyocytes (Figure 6A and 6B). Measurement of cardiomyocyte long-axis length revealed significantly shorter *Rac1*^{SHF} cardiomyocytes compared with littermate control cardiomyocytes (Figure 6E). In addition, neonatal *Rac1*^{SHF} cardiomyocytes were rounded compared with control *Rac1*$^{f/f}$ cardiomyocytes, which had an elongated morphology (Figure 6C and 6D). No rounded cardiomyocytes were found in *Rac1*$^{f/f}$ cultures, whereas >40% of *Rac1*^{SHF} cardiomyocytes exhibited a rounded morphology (Figure 6F). These data strongly support the role of Rac1 in regulating elongation and polarization of cardiomyocytes.

Contribution of SHF Progenitors to *Rac1*^{SHF} Hearts Is Decreased

Histological analysis showed that a deep fissure between the RV and LV was observed in E11.5 *Rac1*^{SHF} hearts, whereas this was not evident and the early muscular interventricular septum was beginning to form in littermate control hearts (Figure 7A and 7B). At E12.5, bifurcation of the RV and LV in *Rac1*^{SHF} hearts continued to be present (Figure 7C and 7D), and by E15.5, a distinct apex was formed in control hearts, whereas *Rac1*^{SHF} hearts continued to have a deep cleft separating the ventricles (Figure 7E and 7F).

Fate mapping with the *mT/mG* global double-fluorescent Cre reporter mouse[18] was performed to follow the developmental progression of the SHF progenitors. A deficiency in the SHF lineage contributing to the developing E11.5 *Rac1*^{SHF}*:mTmG* hearts was evident, especially in the early forming muscular interventricular septum between the RV and LV (Figure 7G and 7H). At E12.5 and E15.5, the interventricular septum in *Rac1*^{SHF}*:mT/mG* hearts had a major deficiency of SHF-derived cells, leading to formation of a bifid apex (Figure 7I and 7L). These findings suggest a critical role for SHF *Rac1* signaling in muscular interventricular septum formation.

Rac1 Promotes Cell Survival in SHF-Derived Myocardium

Aberrant apoptosis or decreased proliferation in the SHF may contribute to CHDs. To determine whether an abnormality in proliferation was a factor in *Rac1*^{SHF} hearts, phosphohistone-H3 protein staining was performed on E11.5 heart sections (Figure 8A through 8F). No differences in proliferation were observed between *Rac1*^{SHF} and *Rac1*$^{f/f}$ control hearts (Figure 8G). Next, we stained for cleaved caspase-3 (the active form of caspase-3) on E11.5 heart sections to detect cell apoptosis (Figure 9A through 9D). Cleaved caspase-3 staining was quantified as a percentage of the total number of cells. E11.5 *Rac1*^{SHF} hearts had significantly higher levels of apoptosis in the RV compared with littermate controls ($P<0.05$) (Figure 9E). Similarly, increased apoptosis was observed in the interventricular septum of E11.5 *Rac1*^{SHF} hearts ($P<0.05$)

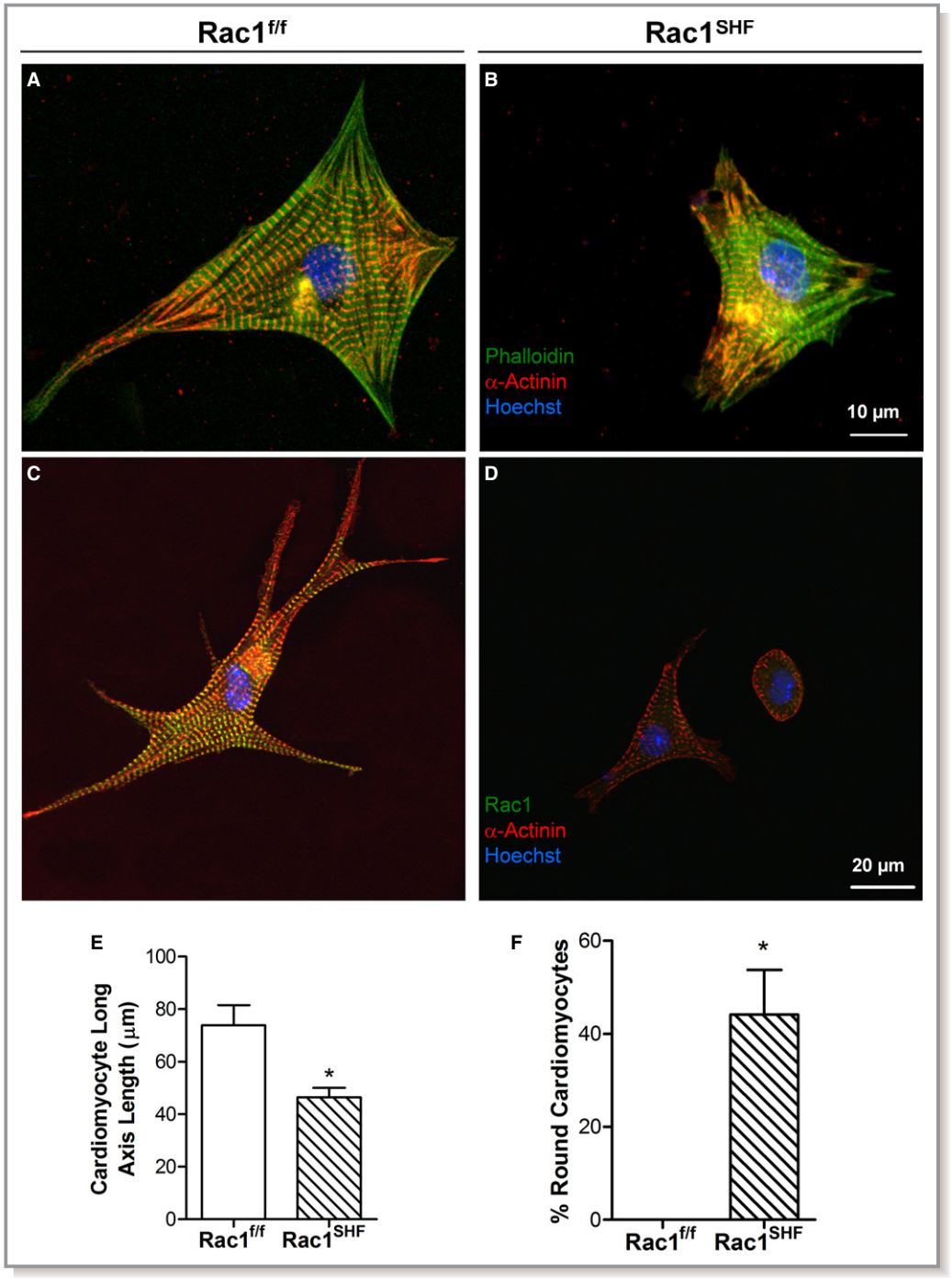

Figure 6. Cells are rounded and cell length is reduced in cultured neonatal *Rac1*^{SHF} cardiomyocytes. A and B, Phalloidin and α-actinin staining of neonatal cardiomyocytes show defective cellular organization and projection formation in *Rac1*^{SHF} cells. C and D, *Rac1*^{SHF} cardiomyocytes are a spherical shape compared with *Rac1*$^{f/f}$ controls. E and F, Long-axis measurements of *Rac1*^{SHF} cardiomyocytes showed that these cells are significantly shorter and more spherical compared with *Rac1*$^{f/f}$ controls. n=3 independent cultures per group, **P*=0.05 by Mann–Whitney test (E). Because penetrance of round cardiomyocyte is 0% in *Rac1*$^{f/f}$ cultures, statistical analysis is not necessary (F). Scale bars: 10 μm (A and B), 20 μm (C and D). SHF indicates second heart field.

(Figure 9B, 9D, and 9E). No significant difference in apoptosis was observed in the LV between E11.5 *Rac1*^{SHF} and control hearts (*P*=0.27) (Figure 9E). Together, these data define a requirement for Rac1 in cell survival but not proliferation in the development of SHF-derived cardiac structures.

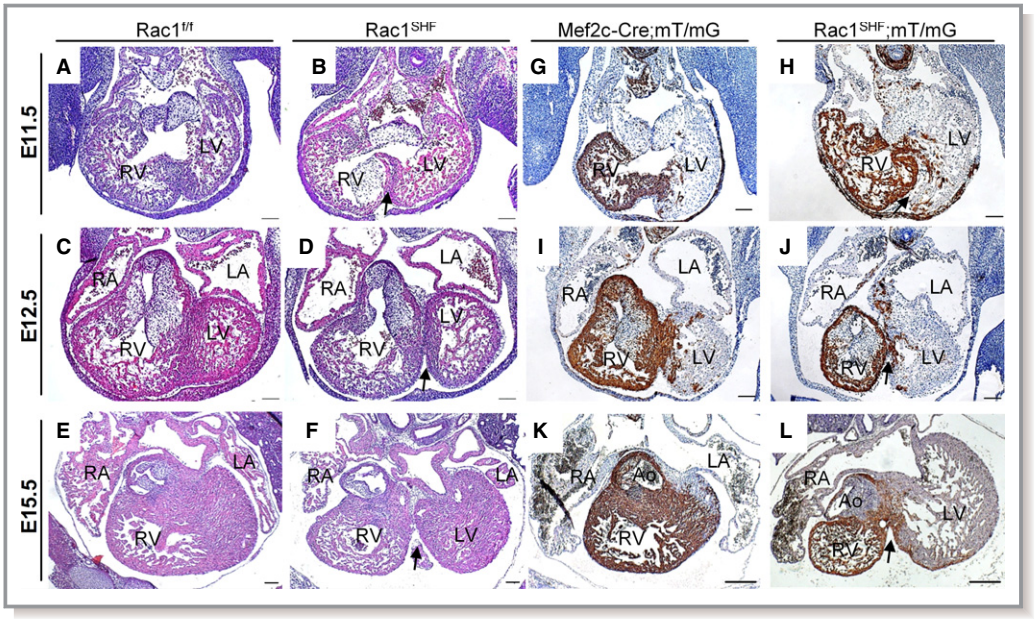

Figure 7. Deficient SHF progenitor contribution to *Rac1*^{SHF} hearts. A through F, hematoxylin and eosin staining of E11.5, E12.5, and E15.5 heart sections shows defective interventricular septum formation (arrow) in *Rac1*^{SHF} hearts, leading to a bifid cardiac apex. G through L, Fate mapping with *mT/mG* reporter shows a decreased SHF progenitor contribution to the interventricular septum (arrow) in *Rac1*^{SHF} hearts. Paraffin sections were immunostained with anti-GFP. Scale bars: 100 μm (A through J), 200 μm (K and L). Ao indicates aorta; GFP, green fluorescent protein; LA indicates left atrium; LV, left ventricle; mG, membrane-targeted GFP; mT, membrane-targeted Tomato; RA, right atrium; RV, right ventricle; SHF, second heart field.

Downregulation of Transcription Factors in *Rac1*^{SHF} RV Myocardium

Heart development is regulated by a complex network of transcription factors that interact synergistically and in a dose-dependent manner to activate target genes.[24] To address the genetic pathways regulated by Rac1 signaling in the SHF, we analyzed known transcription factors important for heart development. Expression levels of *Gata4*, *Nkx2.5*, and *Tbx5* mRNA were significantly decreased in the RV of E13.5 *Rac1*^{SHF} compared with *Rac1*$^{f/f}$ hearts (Table 4). *Hand2* and *Tbx20* are 2 transcription factors shown to be expressed predominantly in the RV and to regulate RV development.[25,26] *Hand2* expression was significantly decreased in the RV of E13.5 *Rac1*^{SHF} compared with *Rac1*$^{f/f}$ hearts (Table 4); however, no significant differences were found in *Tbx20* expression between *Rac1*$^{f/f}$ and *Rac1*^{SHF} RV (Table 4). Taken together, these findings indicate that transcriptional regulation of RV development was severely disrupted in the *Rac1*^{SHF} hearts.

Discussion

The present study was carried out to examine the role of *Rac1* in SHF progenitors. Using the SHF-specific *Mef2c-Cre* mouse line to delete *Rac1* in SHF progenitors and derivatives, we demonstrated that a Rac1 deficiency in the SHF leads to 100% penetrance of CHDs including septal defects, thin RV myocardium, and defective trabeculation and, most notably, a bifid cardiac apex. Our data showed, for the first time, that Rac1 signaling is critical to cardiomyocyte polarity and embryonic heart development, with contributions to cell migration and survival and cardiac gene expression (Figure 9F).

Rac1 has been shown to be a downstream effector of the PCP pathway by modulating the cytoskeleton and regulating actin dynamics in *Drosophila* and *Xenopus*[9,27]; however, the role of Rac1 in mammalian cardiomyocyte polarity and heart development is not known. Studies have shown that disruption of the PCP pathway in mice by deletion of *Scrib* resulted in cellular disorganization, defective trabeculation, thin myocardium, and chamber septation defects,[6] which are strikingly similar to the defects observed in this study and strongly support a disruption of PCP signaling in *Rac1*^{SHF} hearts. Interestingly, we observed that Scrib protein expression pattern is most abundant in the RV and interventricular septum junction during embryonic heart development. Notably, Scrib protein expression in this distinct cardiac tissue area is lost in *Rac1*^{SHF} hearts. We postulate that cardiomyocytes at the RV and interventricular junction must be highly polarized and oriented to align with the forming cardiac apex.

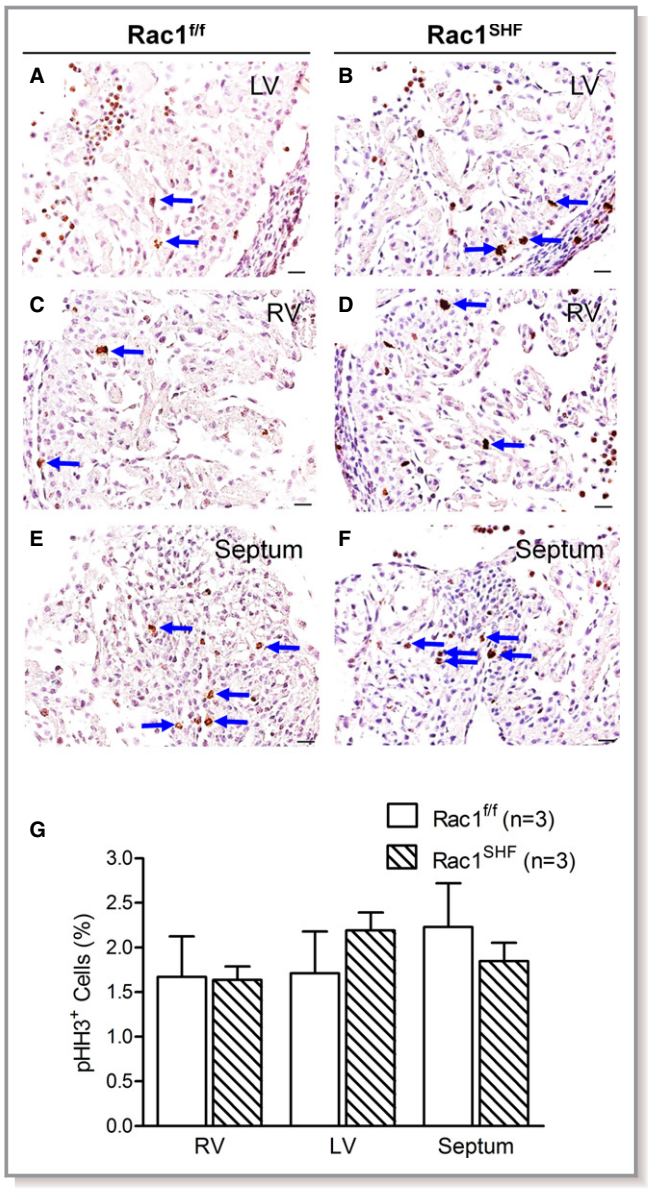

Figure 8. pHH3 protein staining to assess cell proliferation in E11.5 *Rac1*^{SHF} hearts. A through F, Representative pHH3 staining in transverse heart sections. Arrows indicate positive signals. Scale bars: 20 μm. G, No significant differences in cell proliferation were found between E11.5 *Rac1*^{SHF} and *Rac1*$^{f/f}$ hearts. n=3 hearts per group. LV indicates left ventricle; pHH3, phosphohistone-H3; RV, right ventricle; SHF, second heart field.

The rounded, nonpolarized, and disorganized *Rac1*^{SHF} cardiomyocytes are likely unable to bridge the RV and interventricular junction to unify the 2 ventricles to form a cardiac apex, resulting in bifurcation of the muscular septum. In addition, a decrease in cell number due to increases in apoptosis in this area may also contribute to the development of bifid apex. It has been reported that genetic deletion of transcription factor *Ets1* also results in ventricular septal defects and bifid cardiac apex[28]; however, another group using the same *Ets1* knockout mouse did not observe a bifid cardiac apex.[29] This makes the role of *Ets1* still unclear in the formation of a bifid cardiac apex. Recorded cases of bifid cardiac apex in humans are very rare and have usually been reported concomitantly with other congenital heart anomalies including atrial septal defects, ventricular septal defects, and defective RV development,[30,31] which are very similar to the type of defects that were observed in *Rac1*^{SHF} hearts. Consequently, it is possible that the bifid cardiac apex and associated cardiac defects found in humans could be partially associated with abnormalities in *Rac1* signaling and defects in cardiomyocyte polarity during embryonic heart development.

It is well established that actin is the most abundant cytoskeleton protein and plays a critical role in controlling cell orientation, cell shape, and migration. Rac1 is an important regulator of actin polymerization, ruffle formation, lamellipodia extension, and migration in numerous cell types.[7] Rac1 is known to activate the WAVE complex, which is recruited to the plasma membrane and regulates the actin cytoskeleton through the ARP2/3 complex. ARP2/3 associates with actin filaments to promote formation of new filaments from the sides of existing filaments, creating a dendritic network of branched actin filaments to extend lamellipodia and propel cells forward during migration.[32,33] The combined defects in cell polarity, morphology, lamellipodia formation, and actin organization observed in SHF-derived cells led to overall inhibition of cardiomyocyte migratory ability in *Rac1*^{SHF} embryos. Furthermore, Rac1 has been shown to promote cell survival by activation of the PI3K/Akt pathway.[34–36] Decreased migration ability and an increased rate of apoptosis in SHF-derived cells likely to contribute concomitantly to an overall deficiency in SHF contribution to the developing *Rac1*^{SHF} heart.

Numerous studies have found that Rac1 can regulate gene expression through different pathways. Interestingly, it has been shown that Rac1 can activate the canonical Wnt pathway by promoting nuclear accumulation of β-catenin, the effector of the Wnt pathway.[37,38] Ai et al showed that deletion of β-catenin in the SHF led to abnormalities in development of the RV and interventricular septum,[39] very similar to the defects observed in *Rac1*^{SHF} mice in the present study. Whether the defects were also due to loss of β-catenin cell-cell adhesion was not addressed in their study. Our data showed a loss of β-catenin cell adhesions in the *Rac1*^{SHF} RV myocardium, supporting a defect in polarity and placing noncanonical Wnt signaling as the main driver of the cellular and morphological defects observed. Our data are supported by Abhul-Ghani et al, who showed that noncanonical Wnt, which is highly active during cardiogenesis, antagonizes the canonical Wnt pathway.[40] The contribution of canonical Wnt signaling cannot be ruled out in our study because it has been shown to play a role in specification and expansion of early

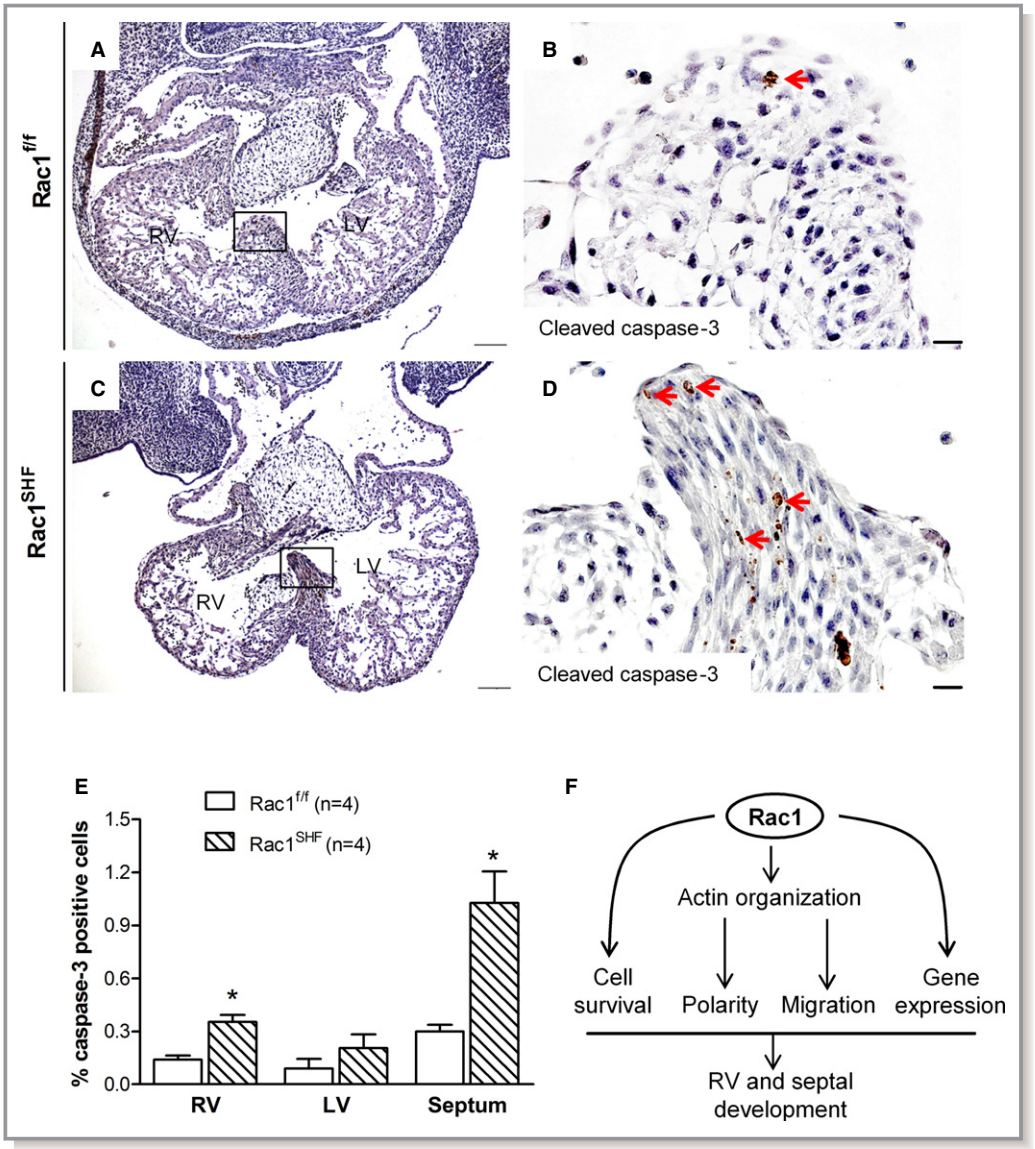

Figure 9. Increased apoptosis in *Rac1*^{SHF} RV and interventricular septum. A through D, E11.5 heart sections were immunostained with cleaved caspase-3 antibody to mark apoptotic cells. Arrows indicate positive signals. B and D are magnifications of the boxes in A and C, respectively. E, Quantification of apoptosis in RV, LV, and the cardiac septum. *P<0.05 vs corresponding Rac1$^{f/f}$ by Mann–Whitney test. Scale bars: 100 μm (A and C), 10 μm (B and D). F, The proposed pathway of Rac1 signaling in SHF derivatives during embryonic heart development. Rac1 regulates actin organization to promote cardiomyocyte polarity and cell migration. In addition, Rac1 promotes cell survival and the expression of cardiac developmental genes. These effects of Rac1 contribute to normal RV and septal development of the heart. LV indicates left ventricle; RV, right ventricle; SHF, second heart field.

SHF progenitors.[41] Rac1 can also promote gene expression through NF-κB and JNK pathways.[42,43] Our data showed that *Rac1*^{SHF} hearts have decreased expression of *Gata4*, *Tbx5*, *Nkx2.5*, and *Hand2* transcription factors in the developing RV. Consequently, it is plausible that a Rac1 deficiency in the SHF will lead to decreased NF-κB and/or JNK signaling and downregulation of key cardiac transcription factors during embryonic heart development. *Tbx20* acts in a dose-sensitive manner as an essential regulator of outflow tract, cardiac valve, and RV development[26]; however, no significant downregulation of *Tbx20* expression was found in the *Rac1*^{SHF} hearts. A hierarchy of distinct cardiac transcription factor regulation exists in the developing heart.[44,45] Our data suggest that Rac1 regulates a distinct network of cardiac transcription factors that do not include *Tbx20* in SHF derivatives. Future studies will be necessary to determine the exact downstream pathways that Rac1 regulates in the SHF to promote cardiac gene expression.

Tbx5 is essential in the SHF for atrial septation,[46] although it is predominantly expressed in the LV during early heart development.[47,48] In addition, Später et al recently challenged the view of Tbx5 as a classical first heart field marker[49]; they showed an overlap of expression pattern between the posterior end of the Tbx5-positive first heart field domain and the Isl1-positive SHF domain, suggesting a role for Tbx5 in the SHF. Our data are compatible with the studies on Tbx5 from Nadeau et al[50] and Xie et al,[46] who showed that Gata4 and Tbx5 cooperatively regulate atrial septum development and that haploinsufficiency of Tbx5 in the SHF results in atrial septal defects.

Although further investigations are required to analyze potential *RAC1* gene mutations in humans with bifid cardiac apex, the present study has shown that SHF *Rac1* is critical to septal and RV development and that deficiencies in SHF Rac1 can give rise to bifid cardiac apex along with the associated CHDs. Our data are the first to show Rac1 as an essential regulator of cardiomyocyte polarity during heart development and to provide a possible mechanism for how bifid cardiac apex arises. Establishment of cellular polarity is essential for the processes regulating cell morphology, lamellipodia formation, and cell migration in the developing embryo, and this seems to be especially critical in formation of a distinct cardiac apex during embryonic heart development.

Sources of Funding

This work was supported in part by operating grants (to Feng) from Canadian Institutes of Health Research (CIHR). Leung was supported by a Natural Sciences and Engineering Research Council (NSERC) Scholarship. Feng is a Heart and Stroke Foundation of Ontario Career Investigator.

Disclosures

None.

References

1. Henderson DJ, Chaudhry B. Getting to the heart of planar cell polarity signaling. *Birth Defects Res A Clin Mol Teratol*. 2011;91:460–467.
2. Niehrs C. The complex world of WNT receptor signalling. *Nat Rev Mol Cell Biol*. 2012;13:767–779.
3. Vivancos V, Chen P, Spassky N, Qian D, Dabdoub A, Kelley M, Studer M, Guthrie S. Wnt activity guides facial branchiomotor neuron migration, and involves the PCP pathway and JNK and ROCK kinases. *Neural Dev*. 2009;4:7.
4. Nagy II, Railo A, Rapila R, Hast T, Sormunen R, Tavi P, Rasanen J, Vainio SJ. Wnt-11 signalling controls ventricular myocardium development by patterning N-cadherin and beta-catenin expression. *Cardiovasc Res*. 2010;85:100–109.
5. Henderson DJ, Phillips HM, Chaudhry B. Vang-like 2 and noncanonical Wnt signaling in outflow tract development. *Trends Cardiovasc Med*. 2006;16:38–45.
6. Phillips HM, Rhee HJ, Murdoch JN, Hildreth V, Peat JD, Anderson RH, Copp AJ, Chaudhry B, Henderson DJ. Disruption of planar cell polarity signaling results in congenital heart defects and cardiomyopathy attributable to early cardiomyocyte disorganization. *Circ Res*. 2007;101:137–145.
7. Heasman SJ, Ridley AJ. Mammalian Rho GTPases: new insights into their functions from in vivo studies. *Nat Rev Mol Cell Biol*. 2008;9:690–701.
8. Munoz-Descalzo S, Gomez-Cabrero A, Mlodzik M, Paricio N. Analysis of the role of the Rac/Cdc42 GTPases during planar cell polarity generation in Drosophila. *Int J Dev Biol*. 2007;51:379–387.
9. Eaton S, Wepf R, Simons K. Roles for Rac1 and Cdc42 in planar polarization and hair outgrowth in the wing of Drosophila. *J Cell Biol*. 1996;135:1277–1289.
10. Sugihara K, Nakatsuji N, Nakamura K, Nakao K, Hashimoto R, Otani H, Sakagami H, Kondo H, Nozawa S, Aiba A, Katsuki M. Rac1 is required for the formation of three germ layers during gastrulation. *Oncogene*. 1998;17:3427–3433.
11. Migeotte I, Omelchenko T, Hall A, Anderson KV. Rac1-dependent collective cell migration is required for specification of the anterior-posterior body axis of the mouse. *PLoS Biol*. 2010;8:e1000442.
12. Kelly RG, Brown NA, Buckingham ME. The arterial pole of the mouse heart forms from Fgf10-expressing cells in pharyngeal mesoderm. *Dev Cell*. 2001;1:435–440.
13. Hutson MR, Kirby ML. Neural crest and cardiovascular development: a 20-year perspective. *Birth Defects Res C Embryo Today*. 2003;69:2–13.
14. Kelly RG. The second heart field. *Curr Top Dev Biol*. 2012;100:33–65.
15. Marelli AJ, Mackie AS, Ionescu-Ittu R, Rahme E, Pilote L. Congenital heart disease in the general population: changing prevalence and age distribution. *Circulation*. 2007;115:163–172.
16. Verzi MP, McCulley DJ, De Val S, Dodou E, Black BL. The right ventricle, outflow tract, and ventricular septum comprise a restricted expression domain within the secondary/anterior heart field. *Dev Biol*. 2005;287:134–145.
17. Glogauer M, Marchal CC, Zhu F, Worku A, Clausen BE, Foerster I, Marks P, Downey GP, Dinauer M, Kwiatkowski DJ. Rac1 deletion in mouse neutrophils has selective effects on neutrophil functions. *J Immunol*. 2003;170:5652–5657.
18. Muzumdar MD, Tasic B, Miyamichi K, Li L, Luo L. A global double-fluorescent Cre reporter mouse. *Genesis*. 2007;45:593–605.
19. Zaffran S, Kelly RG, Meilhac SM, Buckingham ME, Brown NA. Right ventricular myocardium derives from the anterior heart field. *Circ Res*. 2004;95:261–268.
20. Liu Y, Lu X, Xiang FL, Lu M, Feng Q. Nitric oxide synthase-3 promotes embryonic development of atrioventricular valves. *PLoS One*. 2013;8:e77611.
21. Song W, Lu X, Feng Q. Tumor necrosis factor-alpha induces apoptosis via inducible nitric oxide synthase in neonatal mouse cardiomyocytes. *Cardiovasc Res*. 2000;45:595–602.
22. Raftopoulou M, Hall A. Cell migration: Rho GTPases lead the way. *Dev Biol*. 2004;265:23–32.
23. Eden S, Rohatgi R, Podtelejnikov AV, Mann M, Kirschner MW. Mechanism of regulation of WAVE1-induced actin nucleation by Rac1 and Nck. *Nature*. 2002;418:790–793.
24. Bruneau BG. The developmental genetics of congenital heart disease. *Nature*. 2008;451:943–948.
25. Thomas T, Yamagishi H, Overbeek PA, Olson EN, Srivastava D. The bHLH factors, dHAND and eHAND, specify pulmonary and systemic cardiac ventricles independent of left-right sidedness. *Dev Biol*. 1998;196:228–236.
26. Takeuchi JK, Mileikovskaia M, Koshiba-Takeuchi K, Heidt AB, Mori AD, Arruda EP, Gertsenstein M, Georges R, Davidson L, Mo R, Hui CC, Henkelman RM, Nemer M, Black BL, Nagy A, Bruneau BG. Tbx20 dose-dependently regulates transcription factor networks required for mouse heart and motoneuron development. *Development*. 2005;132:2463–2474.
27. Habas R, Dawid IB, He X. Coactivation of Rac and Rho by Wnt/Frizzled signaling is required for vertebrate gastrulation. *Genes Dev*. 2003;17:295–309.
28. Ye M, Coldren C, Liang X, Mattina T, Goldmuntz E, Benson DW, Ivy D, Perryman MB, Garrett-Sinha LA, Grossfeld P. Deletion of ETS-1, a gene in the Jacobsen syndrome critical region, causes ventricular septal defects and abnormal ventricular morphology in mice. *Hum Mol Genet*. 2010;19:648–656.
29. Gao Z, Kim GH, Mackinnon AC, Flagg AE, Bassett B, Earley JU, Svensson EC. Ets1 is required for proper migration and differentiation of the cardiac neural crest. *Development*. 2010;137:1543–1551.
30. Sayin OA, Ugurlucan M, Dursun M, Ucar A, Tireli E. Bifid cardiac apex: a rare morphologic structure. *J Thorac Cardiovasc Surg*. 2006;131:474–475.
31. Teja K, Sturgill BC. Bifid cardiac apex. *Am Heart J*. 1986;111:1004–1005.
32. Millard TH, Sharp SJ, Machesky LM. Signalling to actin assembly via the WASP (Wiskott-Aldrich syndrome protein)-family proteins and the Arp2/3 complex. *Biochem J*. 2004;380:1–17.

33. Stradal TE, Rottner K, Disanza A, Confalonieri S, Innocenti M, Scita G. Regulation of actin dynamics by WASP and WAVE family proteins. *Trends Cell Biol*. 2004;14:303–311.
34. Jiang K, Zhong B, Ritchey C, Gilvary DL, Hong-Geller E, Wei S, Djeu JY. Regulation of Akt-dependent cell survival by Syk and Rac. *Blood*. 2003;101:236–244.
35. Nishida K, Kaziro Y, Satoh T. Anti-apoptotic function of Rac in hematopoietic cells. *Oncogene*. 1999;18:407–415.
36. Gonzalez E, Kou R, Michel T. Rac1 modulates sphingosine 1-phosphate-mediated activation of phosphoinositide 3-kinase/Akt signaling pathways in vascular endothelial cells. *J Biol Chem*. 2006;281:3210–3216.
37. Esufali S, Bapat B. Cross-talk between Rac1 GTPase and dysregulated Wnt signaling pathway leads to cellular redistribution of beta-catenin and TCF/LEF-mediated transcriptional activation. *Oncogene*. 2004;23:8260–8271.
38. Wu X, Tu X, Joeng KS, Hilton MJ, Williams DA, Long F. Rac1 activation controls nuclear localization of beta-catenin during canonical Wnt signaling. *Cell*. 2008;133:340–353.
39. Ai D, Fu X, Wang J, Lu MF, Chen L, Baldini A, Klein WH, Martin JF. Canonical Wnt signaling functions in second heart field to promote right ventricular growth. *Proc Natl Acad Sci USA*. 2007;104:9319–9324.
40. Abdul-Ghani M, Dufort D, Stiles R, De Repentigny Y, Kothary R, Megeney LA. Wnt11 promotes cardiomyocyte development by caspase-mediated suppression of canonical Wnt signals. *Mol Cell Biol*. 2011;31:163–178.
41. Cohen ED, Wang Z, Lepore JJ, Lu MM, Taketo MM, Epstein DJ, Morrisey EE. Wnt/beta-catenin signaling promotes expansion of Isl-1-positive cardiac progenitor cells through regulation of FGF signaling. *J Clin Invest*. 2007;117:1794–1804.
42. Arbibe L, Mira JP, Teusch N, Kline L, Guha M, Mackman N, Godowski PJ, Ulevitch RJ, Knaus UG. Toll-like receptor 2-mediated NF-kappa B activation requires a Rac1-dependent pathway. *Nat Immunol*. 2000;1:533–540.
43. Coso OA, Chiariello M, Yu JC, Teramoto H, Crespo P, Xu N, Miki T, Gutkind JS. The small GTP-binding proteins Rac1 and Cdc42 regulate the activity of the JNK/SAPK signaling pathway. *Cell*. 1995;81:1137–1146.
44. Klaus A, Muller M, Schulz H, Saga Y, Martin JF, Birchmeier W. Wnt/beta-catenin and Bmp signals control distinct sets of transcription factors in cardiac progenitor cells. *Proc Natl Acad Sci USA*. 2012;109:10921–10926.
45. Mandel EM, Kaltenbrun E, Callis TE, Zeng XX, Marques SR, Yelon D, Wang DZ, Conlon FL. The BMP pathway acts to directly regulate Tbx20 in the developing heart. *Development*. 2010;137:1919–1929.
46. Xie L, Hoffmann AD, Burnicka-Turek O, Friedland-Little JM, Zhang K, Moskowitz IP. Tbx5-hedgehog molecular networks are essential in the second heart field for atrial septation. *Dev Cell*. 2012;23:280–291.
47. Bruneau BG, Logan M, Davis N, Levi T, Tabin CJ, Seidman JG, Seidman CE. Chamber-specific cardiac expression of Tbx5 and heart defects in Holt-Oram syndrome. *Dev Biol*. 1999;211:100–108.
48. Li QY, Newbury-Ecob RA, Terrett JA, Wilson DI, Curtis AR, Yi CH, Gebuhr T, Bullen PJ, Robson SC, Strachan T, Bonnet D, Lyonnet S, Young ID, Raeburn JA, Buckler AJ, Law DJ, Brook JD. Holt-Oram syndrome is caused by mutations in TBX5, a member of the Brachyury (T) gene family. *Nat Genet*. 1997;15:21–29.
49. Spater D, Abramczuk MK, Buac K, Zangi L, Stachel MW, Clarke J, Sahara M, Ludwig A, Chien KR. A HCN4+ cardiomyogenic progenitor derived from the first heart field and human pluripotent stem cells. *Nat Cell Biol*. 2013;15:1098–1106.
50. Nadeau M, Georges RO, Laforest B, Yamak A, Lefebvre C, Beauregard J, Paradis P, Bruneau BG, Andelfinger G, Nemer M. An endocardial pathway involving Tbx5, Gata4, and Nos3 required for atrial septum formation. *Proc Natl Acad Sci USA*. 2010;107:19356–19361.